

# Influence of doping and substrate type on the metastable phase growth in pulsed-laser evaporated PbTe films

M. BALEVA, E. MATEEVA

*Faculty of Physics, Sofia University, 1126 Sofia, Bulgaria*

PbTe films, undoped and doped with 0.02, 0.3 mol % Cr and 0.02 mol % Co, grown by pulsed-laser evaporation (PLE) on different types of substrates have been investigated. The crystal structure of the films was studied by X-ray diffraction. Along with the stable fcc phase, metastable GeS- and CsCl-type phases of PbTe were detected in the films. The growth of the metastable phases as well as the influence of the substrate type and temperature and the doping on the growth have been analyzed in the framework of the classical thermodynamic theory of crystallization. It was found that the influence of doping consists in the change of the surface free energy of the deposited material, while the substrate-type influence depends on its linear thermal expansion coefficient—when it is equal to that of the deposited compound the substrate stimulates the growth of the metastable phases. It is concluded that the growth mechanism is graphoepitaxy.

## 1. Introduction

Our investigations of PbTe and PbSe films have shown that films with the metastable phases of these materials grow spontaneously at a high rate of supercooling when deposited by non-equilibrium techniques such as pulsed-laser evaporation (PLE) [1]. PbTe and PbSe, which at ambient conditions crystallize into the NaCl-type fcc structure, are known to possess two high-pressure (HP) metastable phases: orthorhombic (GeS-type PbTe and TII-type PbSe) and CsCl-type [2–4]. The growth of these structures leads to important electronic consequences, including formation of novel materials with new band gaps and tailoring new structures. We have shown that the CsCl-type and the orthorhombic phases of PbTe and PbSe have qualitatively different properties from those of PbTe and PbSe grown in the bulk form, i.e. in the stable fcc phase [5–9]. The energy gap of PbTe with CsCl-type structure, for example, is  $E_g^{\text{CsCl}} = 0.23$  eV (300 K), while that of fcc PbTe is  $E_g^{\text{fcc}} = 0.32$  eV (300 K). On the other hand, the films grown by PLE were found to represent heterophase junctions between a sublayer with metastable phases and a sublayer with the stable phase.

The thickness of the sublayers with the metastable phases is of the order of micrometres and can be attributed neither to the lattice coherence with the substrate nor to the change of stoichiometry. We have shown that the growth of metastable phases is spontaneous and is governed by the high rate of supercooling in the non-equilibrium techniques [1], in other words, it is a matter of growth dynamics. In the present work our aim was semiquantitatively to consider the influence of doping and substrate type on the

growth process. This comprehensive study of the influence of technological parameters on the growth of the metastable phases is important, in that it concerns tailoring of the heterophase junctions.

## 2. Experimental procedure and results

### 2.1. Samples

PbTe and PbTe doped with 0.02, 0.3 mol % Cr and 0.02 mol % Co films were grown by PLE. The apparatus for the technical realization of PLE was described elsewhere [10]. The technological parameters, which are varied in this technique, are substrate temperature,  $T_s$ , substrate-to-target distance,  $L$ , laser pulse energy,  $E_j$ , number of laser pulses,  $N$ . All the investigated films were deposited with laser pulse energy  $E_j = 2$ –3 J per pulse and  $L = 3$  cm. The films investigated were comparatively thin in order to contain predominantly metastable phases. It was shown earlier [1] that the thickness of the metastable phase sublayer on KCl substrates reaches about 0.7  $\mu\text{m}$  and that further growth is with the stable fcc phase. The thicknesses of the samples were determined from the pictures of the cross-sections taken with a scanning electron microscope. The substrate temperature was maintained at different temperatures in the range of 50–300 °C. Pairs of films were deposited simultaneously on (100)-oriented KCl and KBr substrates to provide identical technological conditions to determine the effect of the substrate type on the formation of the metastable phases. The monocrystalline KCl, KBr and BaF<sub>2</sub> substrates were freshly cut from large single crystals in their most easily cleaved directions – (100) for KCl and KBr, and (111) for BaF<sub>2</sub> – which ensures a

periodic surface morphology of these substrates. The lattice constants of KCl and KBr are different:  $a_{\text{KCl}} = 0.6293 \text{ nm}$  (300 K) and  $a_{\text{KBr}} = 0.6597 \text{ nm}$  (300 K). The linear thermal expansion coefficients,  $\alpha$ , of KCl and KBr differ from one another and are quite different from that of PbTe (Fig. 1) (see, for example, [11, 12]). In order to obtain a more complete study of the role of substrate type, some films were deposited on (111)-oriented  $\text{BaF}_2$  ( $a_{\text{BaF}_2} = 0.6200 \text{ nm}$ , 300 K) and on glass substrates. The linear thermal expansion coefficient of the  $\text{BaF}_2$  substrate as seen from Fig. 1 is

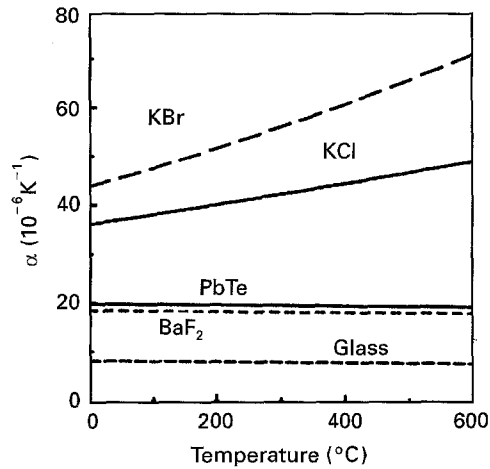


Figure 1 Temperature dependences of the linear thermal expansion coefficients of the substrate materials and the deposited material – PbTe [11, 12].

close to that of PbTe. The samples are specified in Tables I and II. In the labelling of the samples, K represents the KCl substrate, KB the KBr substrate, B the  $\text{BaF}_2$  substrate, G the glass substrate, and T PbTe; CR signifies that the samples are doped with Cr and the following number shows the amount of dopant (for example CR3 means that the film is doped with 0.3 mol % Cr).

## 2.2. X-ray investigations

The crystal structure of the films was investigated by X-ray diffraction. The X-ray diffraction patterns were obtained by a standard X-ray diffractometer Philips-PW1040 with  $\text{CoK}_\alpha$  radiation with graphite monochromator and velocity of  $2^\circ \text{ min}^{-1}$ . The angular range was varied from  $20^\circ$ – $80^\circ$ . The lattice constants and the peak intensities were obtained using the PULVERIX program as implemented by H. Moller, Institut für Experimental Physik, Technische Universität, 1040 Wien, Austria. Fig. 2 shows the typical X-ray diffraction patterns for an undoped (K20T), doped with 0.3 mol % Cr (CR3K23T) and 0.02 mol % Co (CO02K30T) PbTe films deposited on KCl substrates. Fig. 3 shows the X-ray diffraction patterns of undoped PbTe films deposited simultaneously on KCl (K20T), KBr (KB1T) and  $\text{BaF}_2$  (B26T) substrates.

The most intensive peaks in all these diffractograms, except for the film grown on the  $\text{BaF}_2$  substrate, indicate monocrystal fcc NaCl-type structure with (100) orientation. The values of the fcc PbTe phase

TABLE I Lattice constants of PbTe crystal phases and the lattice volume changes of PbTe HP metastable phases  $V/V_0$ .  $V_0 = 0.2693 \text{ nm}^3$  is the fcc volume at  $T = 300 \text{ K}$  and  $P = 5 \text{ kbar}$  [3]

Samples	Substrate	Doping (mol %)	Lattice constants (nm)					$V/V_0$	
			GeS-type			CsCl-type	NaCl-type	GeS-type	CsCl-type
			a	b	c	a	a		
K20T	KCl	–	0.4341	1.1650	0.4405	0.3565	0.6432	0.827	0.710
K25T	KCl	–	0.4377	1.1712	0.4359	0.3587	0.6441	0.833	0.724
K27T	KCl	–	–	–	–	0.3586	0.6441	–	0.724
KB1T	KBr	–	–	–	–	0.3608	0.6443	–	0.739
KB17T	KBr	–	0.4739	1.1476	0.4332	0.3570	0.6452	0.877	0.717
KB15T	KBr	–	–	–	–	0.3571	0.6452	–	0.717
B26T	$\text{BaF}_2$	–	0.4510	1.1359	0.4217	0.3532	0.6554	0.800	0.690
B28T	$\text{BaF}_2$	–	0.4523	1.1240	0.4181	0.3540	0.6556	0.754	0.707
G17T	Glass	–	–	–	–	–	0.6479	–	–
G13T	Glass	–	–	–	–	–	0.6479	–	–
			Cr						
CR02K21T	KCl	0.02	0.4692	1.1572	0.4322	0.3562	0.6432	0.870	0.710
CR02K19T	KCl	0.02	–	–	–	0.3587	0.6432	–	0.726
CR02KB14T	KBr	0.02	–	–	–	0.3582	0.6443	–	0.725
CR02KB2T	KBr	0.02	–	–	–	0.3568	0.6442	–	0.715
CR3K24T	KCl	0.3	0.5090	1.0840	0.4577	0.3583	0.6433	0.930	0.725
CR3K23T	KCl	0.3	0.5048	1.0810	0.4537	0.3561	0.6433	0.910	0.710
CR3K22T	KCl	0.3	0.4684	1.1568	0.4329	0.3559	0.6433	0.870	0.710
CR3KB3T	KBr	0.3	0.4662	1.1644	0.4449	0.3572	0.6440	0.893	0.718
CR3KB13T	KBr	0.3	–	–	–	0.3588	0.6440	–	0.727
CR3KB4T	KBr	0.3	–	–	–	0.3582	0.6440	–	0.724
			Co						
CO02K29T	KCl	0.02	0.4683	1.1572	0.4348	0.3570	0.6447	0.875	0.716
CO02K30T	KCl	0.02	–	–	–	0.3572	0.6447	–	0.716
CO02KB9T	KBr	0.02	–	–	–	0.3573	0.6447	–	0.716
CO02KB10T	KBr	0.02	–	–	–	0.3571	0.6447	–	0.716

TABLE II Ratios of the intensities  $I_{200}^{\text{CsCl}}$  and  $I_{100}^{\text{CsCl}}$  of the CsCl-type phase (200) and (100) reflections and the intensities  $I_{042}^{\text{GeS}}$  and  $I_{120}^{\text{GeS}}$  of GeS-type phase (042) and (120) reflections, determined from the experimental diffraction patterns as a function of the substrate temperature,  $T_s$ , and type, and the doping

Samples	Substrate	Doping (mol %)	$T_s$ (°C)	$\frac{I_{200}^{\text{CsCl}}}{I_{042}^{\text{GeS}}}$	$\frac{I_{100}^{\text{CsCl}}}{I_{120}^{\text{GeS}}}$
K20T	KCl	–	200	0.8	–
K25T	KCl	–	250	3.8	–
K27T	KCl	–	150	0.7	–
KB1T	KBr	–	200	–	0.8
KB17T	KBr	–	250	–	0.9
KB15T	KBr	–	150	–	–
		Cr			
CR02K21T	KCl	0.02	300	0.6	–
CR02K19T	KCl	0.02	50	0.7	–
CR02KB14T	KBr	0.02	200	–	1.9
CR02KB2T	KBr	0.02	50	–	0.5
CR3K24T	KCl	0.3	300	3.0	–
CR3K23T	KCl	0.3	200	3.1	–
CR3K22T	KCl	0.3	50	4.2	–
CR3KB3T	KBr	0.3	300	–	2.6
CR3KB13T	KBr	0.3	200	–	4.3
CR3KB4T	KBr	0.3	50	–	8.0
		Co			
CO02K29T	KCl	0.02	50	2.0	–
CO02K30T	KCl	0.02	200	2.0	–
CO02KB9T	KBr	0.02	50	→ ∞	–
CO02KB10T	KBr	0.02	300	→ ∞	–

lattice parameter,  $a$ , determined from the diffractograms are given in Table I. These values vary from 0.6441–0.6452 nm. This variation corresponds to a change in the pressure  $\Delta P = 3$  kbar, as follows from the pressure dependence of the lattice volumes  $[V_1/V_0(P)]$  of the three PbTe phases, obtained by Chattopadhyay *et al.* [3] (reproduced in Fig. 4). The additional reflections in the diffractograms, are indexed into the two HP PbTe phases, growing in the initial stage of deposition of the films, forming the sublayer adjacent to the substrate [1]. These reflections arise from the polycrystal GeS- and CsCl-type phases. The CsCl-type phase is found to crystallize with (100) orientation in the undoped and doped films deposited on KBr substrates, and in the undoped and 0.02 mol % Cr doped films grown on KCl and BaF<sub>2</sub> substrates. In PbTe/KCl films doped with 0.3 mol % Cr and 0.02 mol % Co, the (110) reflection of the CsCl-type phase is detected. The ratio of the intensities of the (100) and (110) reflections of this phase in the calculated polycrystal X-ray spectrum is  $I_{(100)}^{\text{CsCl}}/I_{(110)}^{\text{CsCl}} = 0.056$ . The same ratio determined from the experimental spectra is  $I_{(100)}^{\text{CsCl}}/I_{(110)}^{\text{CsCl}} = 1.25$ –2. The latter indicates that the CsCl-type phase in the films doped with 0.3 mol % Cr and 0.02 mol % Co on KCl substrates also grows predominantly with (100) orientation. The lattice parameters  $a$ ,  $b$  and  $c$  of the orthorhombic GeS-type phase, as well as the lattice constant,  $a$ , of the CsCl-type phase, determined from the X-ray diffraction patterns for all investigated samples, are given in Table I. In Figs 2 and 3 the experimental X-ray spectra are compared with the calculated ones. The solid vertical bars represent the intensities of the reflections of the (100) fcc, the (100)

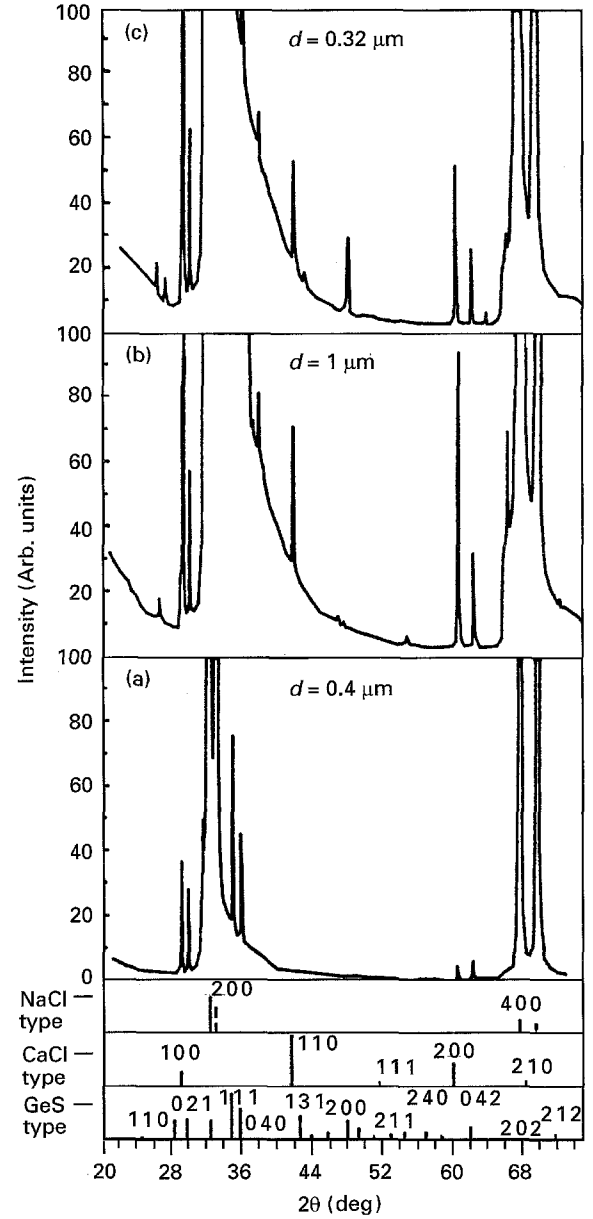


Figure 2 X-ray diffraction patterns of (a) undoped (K20T), doped with (b) 0.3 mol % Cr (CR3K23T) and (c) 0.02 mol % Co (CO02K30T) PbTe films deposited on KCl substrates. The solid vertical bars represent the intensities of the reflections of the (100) fcc, the polycrystal CsCl-type and the polycrystal orthorhombic GeS-type phases of PbTe. The dashed vertical bars show the intensities of the reflections of the monocrystal (100) KCl substrate.

CsCl-type and the polycrystal orthorhombic GeS-type phases. In Fig. 2 the intensities of the reflections of the polycrystal CsCl-type phase are shown. The dashed vertical bars in Fig. 2 show the intensities of the reflections of the KCl substrate. In Fig. 3, the intensities of the reflections of the three different substrates are given in the experimental spectra. The intensities of the reflections of the polycrystal GeS-type phase are calculated assuming the same positions of the lead and tellurium atoms as those in SnSe, in the way done by Fujii *et al.* [2] and with the parameters  $a$ ,  $b$  and  $c$  for sample B26T (see Table I). The intensities of the reflections of the CsCl-type phase are calculated with the parameter  $a$  of sample B26T.

In the X-ray diffraction patterns of the undoped PbTe films deposited on BaF<sub>2</sub> substrates, Fig. 3,

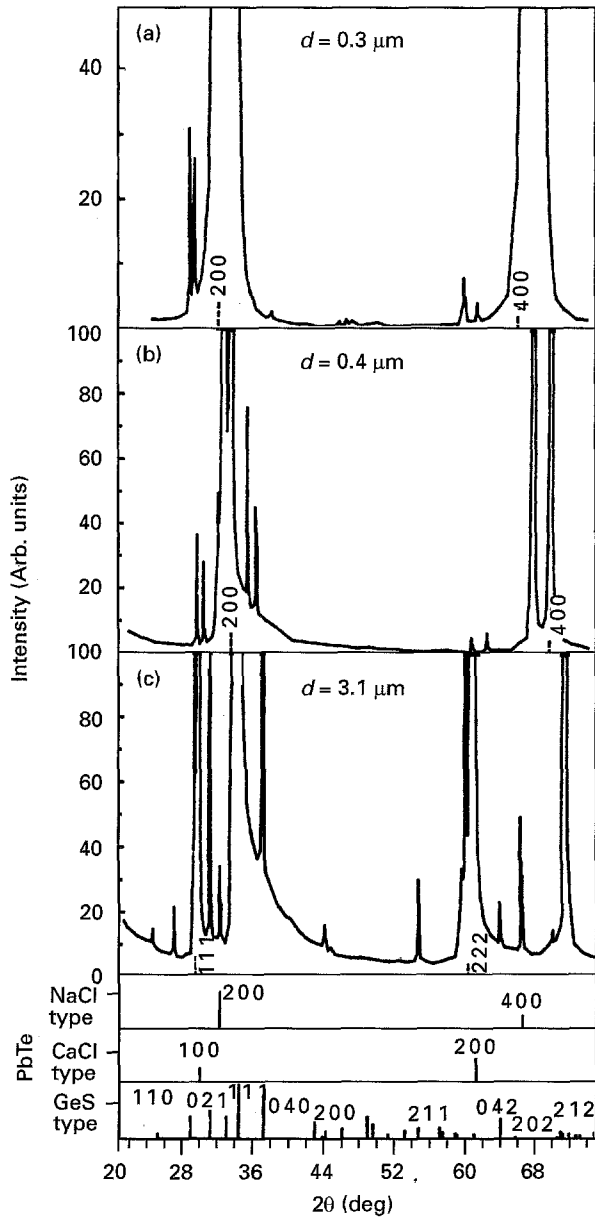


Figure 3 X-ray diffraction patterns of undoped PbTe films deposited simultaneously on (a) KBr (KB1T), (b) KCl (K20T) and (c) BaF<sub>2</sub> (B26T) substrates. The solid vertical bars represent the intensities of the reflections of the (100) fcc, the (100) CsCl-type and the polycrystal orthorhombic GeS-type phases. (---) The intensities of the reflections of the three different substrates.

sample B26T, the reflections of the HP phases are much more intensive than those of the stable fcc phase. The latter allows the (111) reflections of the GeS-type phase, hidden in the diffraction patterns of the other films by the strong (200) fcc PbTe and KCl and KBr substrate reflections, to be seen. The lattice parameters of the CsCl-type structure ( $a = 0.3532$  nm) and GeS-type phase ( $a = 0.4510$  nm,  $b = 1.1359$  nm and  $c = 0.4217$  nm) in the films deposited on BaF<sub>2</sub> substrates are smaller compared to those determined in the films grown on KCl and KBr substrates.

Fig. 5 shows the X-ray diffraction patterns of undoped PbTe films (G17T, G13T) deposited on glass substrates. The diffraction patterns of these films like those deposited on KCl and KBr substrates, also indicate mainly monocrystal NaCl-type PbTe structure with (100) orientation. Additional reflections are

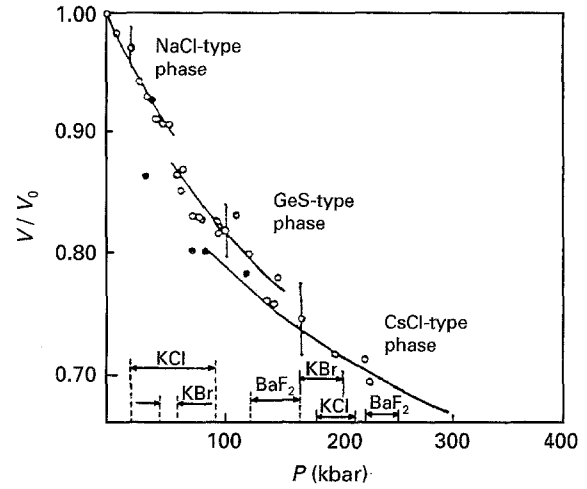


Figure 4 Pressure-induced change of the lattice volume of the different PbTe phases, obtained by Chattopadhyay *et al.* [4]. The regions of the CsCl- and GeS-type phases volume changes in the films grown on different substrates are indicated.

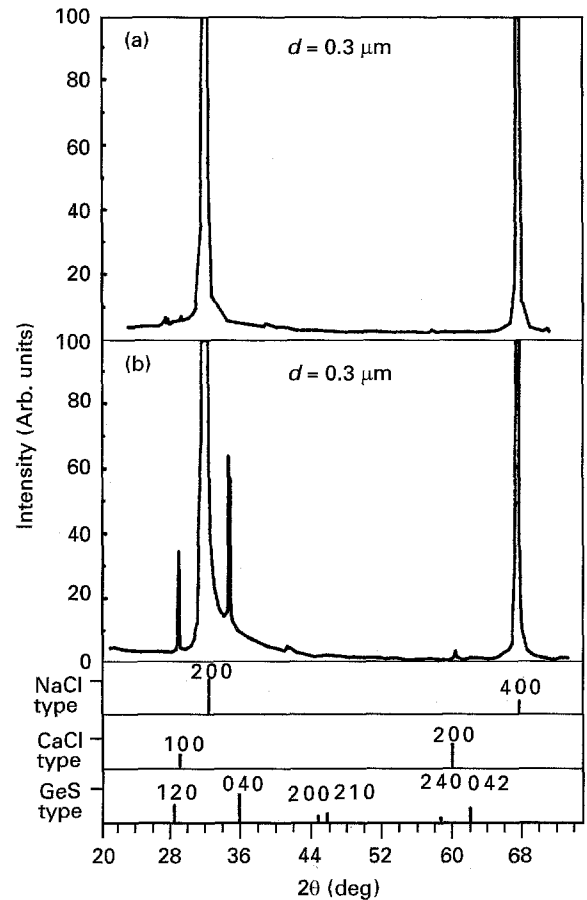


Figure 5 X-ray diffraction patterns of (a) G13T and (b) G17T PbTe films deposited on amorphous glass substrates at (b) 150 and (a) 250 °C.

seen only in the diffractogram of the sample deposited at  $T_s = 150$  °C. These reflections can be indexed into the polycrystal GeS-type phase but they are not enough for all three lattice parameters of this phase to be determined. In the film deposited at  $T_s = 250$  °C, reflections of the metastable phases can hardly be resolved. Then the quantity of the metastable phases, if any, in this film is negligible.

The lattice volumes of the HP phases in the various samples are calculated from the corresponding lattice parameters and are given in Table I. The lattice volume variations for the GeS- and the CsCl-type phases in the samples deposited on different substrates are shown in Fig. 4. It can be seen that in the films deposited on BaF<sub>2</sub> substrates, the CsCl- and the GeS-type phases volume changes correspond to the highest hydrostatic pressures.

The change of the relative content of the two HP phases from one sample to another can be followed by comparing the intensity of a reflection of one metastable phase to that of the other. The ratios of the intensities of the (100) CsCl-type phase and the (120) GeS-type phase,  $I_{(1\ 0\ 0)}^{\text{CsCl}}/I_{(0\ 2\ 1)}^{\text{GeS}}$ , or the ratio  $I_{(2\ 0\ 0)}^{\text{CsCl}}/I_{(0\ 4\ 2)}^{\text{GeS}}$  in the films, where these ratios can be determined, are given in Table II. The trend of increasing GeS-type phase relative to the CsCl-type phase with temperature rise, confirms the results reported recently [1, 7].

### 3. Discussion

The growth mechanism of the metastable phases and the heterophase films can be understood in the framework of the classical crystallization theory. The nucleation rate for the two-dimensional nucleus formation is given by [13, 14]

$$J = Zv_0 N_0 \exp\left[\frac{-4a^2s^2}{\Delta H \Delta T/T_m - a^2 \Delta \sigma} \frac{1}{kT} - \frac{U}{kT}\right] \quad (1)$$

where  $Z$  is the so-called Zeldovich factor, which varies between 0.1 and 1,  $v_0$  is the surface-vibrational frequency of the adatoms,  $N_0$  is the density of the absorption sites on the substrate,  $k$  is the Boltzmann constant,  $T$  is the temperature (the substrate temperature,  $T_s$ , in our case), and  $U$  is the activation energy for a surface diffusion of adatoms from a regular to an irregular site.  $\Delta H$  is the enthalpy change,  $a$  is the atomic diameter,  $s$  is the specific periphery edge free energy and  $\Delta \sigma = \sigma + \sigma_i - \sigma_s$  is the change of the specific surface free energy and  $\sigma$ ,  $\sigma_i$  and  $\sigma_s$  are the specific surface free energies of the deposit, of the deposit-substrate interface and of the substrate.  $\Delta T = T_m - T$  is the supercooling and  $T_m$  is the material melting temperature.

This equation is valid for the nucleation of a one-component material. The stoichiometry of laser-deposited thin films reproduces the target stoichiometry because of the high speed of the particles condensing on the substrate. Thus we can use Equation 1 to analyse the influence of the substrate temperature and type, and of the doping on the growth mechanism of PbTe films.

We have shown in the case of PbTe/KCl films that the main reason for the growth of metastable phases is the high rate of supercooling in the non-equilibrium process of growth [1]. The low substrate temperature is the main factor determining the thermodynamics of the growth mechanism. The latter is easily seen from the solid curves in Figs 6 and 7 which represent the nucleation rate temperature dependences of the three

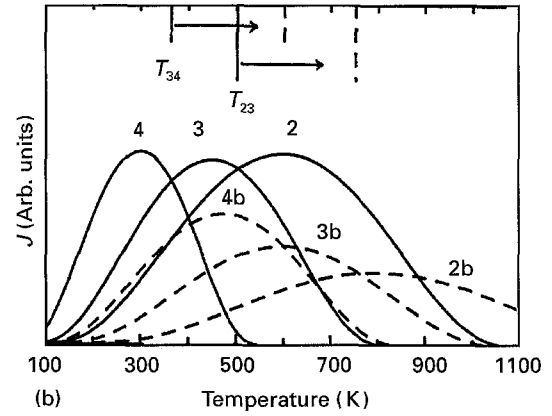
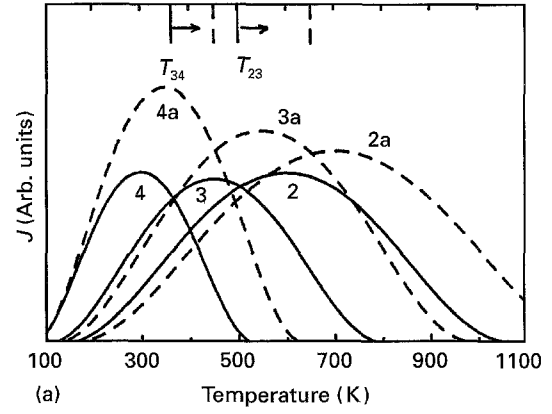


Figure 6 Comparison of the nucleation rate temperature dependences, calculated according to Equation 1 with (—)  $\Delta \sigma = 0$  and (---) with (a)  $\Delta \sigma_{\text{Cr}} < 0$  and  $s_{\text{Cr}} < s$  of the undoped films, and (b)  $\Delta \sigma_{\text{Co}} < \Delta \sigma_{\text{Cr}}$  and  $s_{\text{Co}} < s_{\text{Cr}}$ . All curves were calculated with  $U = 0$ .

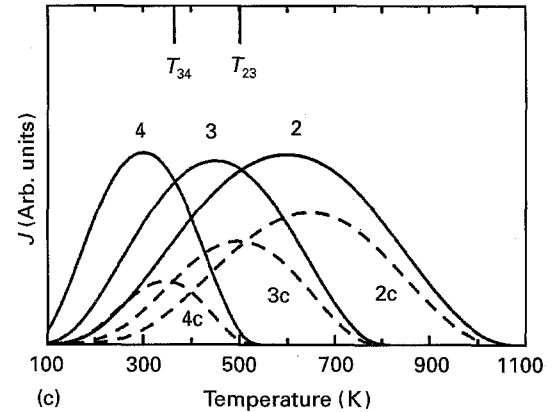


Figure 7 Comparison of the nucleation rate temperature dependences, calculated according to Equation 1, with  $U =$  (—) 0 and (---)  $> 0$ . All curves were calculated with  $\Delta \sigma = 0$ .

different PbTe phases (curve 2 holds for the stable phase, curve 3 for the GeS-type phase, and curve 4 for the CsCl-type phase). These dependences are calculated according to Equation 1 with  $\Delta \sigma = 0$  and  $U = 0$  and with different melting temperatures for the three phases. The melting temperature of the stable fcc phase,  $T_{m2} = 1197$  K, i.e. the critical temperature of the transition from the liquid phase 1 to the solid phase 2 is known. The unknown melting temperatures of the two metastable phases are assumed to be  $T_{m3} = 900$  K for the intermediate GeS-type phase and

$T_{m4} = 600$  K for the CsCl-type phase. It is seen from the solid curves in Figs 6 and 7 that at substrate temperature  $T_s < T_{34}$  the possibility of growing the metastable phase 4 (CsCl-type phase) is highest, at  $T_{34} < T_s < T_{23}$  the metastable phase 3 (GeS-type phase) is most probable, and at  $T_s > T_{23}$ , the formation of the stable fcc phase takes place.

The overall film crystal structure can be understood if one assumes the crystallization front temperature to increase from pulse to pulse. The substrate temperatures used in the experiment obviously are lower than  $T_{34}$  as far as the CsCl-type phase, although in different quantities, is detected in all the films. When the crystallization front temperature, increasing from pulse to pulse, becomes comparable with  $T_{34}$ , the probability of growing the GeS-type phase prevails. It is clear that the number of the laser pulses necessary to reach the temperature  $T_{34}$  depends on the substrate temperature. The lower the substrate temperature, the higher is the number of the pulses and the thicker is the sublayer with the CsCl-type phase. On increasing the substrate temperature, the relative quantity of the GeS-type phase increases so that at  $T_s > 200$  °C it dominates. At a certain number of laser pulses, which means certain critical thickness,  $d_m$ , the crystallization front temperature reaches  $T_{23}$  and the stable fcc phase grows. When the thickness of the sublayer with one of the metastable phases is comparable with the stable phase sublayer the film becomes a heterophase junction which is a new type of semiconductor structure.

### 3.1. Influence of doping

It is seen from the X-ray diffraction patterns, Fig. 2, that the CsCl-type phase is more dominant in the doped films. This means that the temperature  $T_{34}$  for these materials is shifted to higher temperatures and thus the growth of the CsCl-type phase can take place over a larger range of substrate temperatures. The influence of doping can be sought in the change of the periphery surface energy and the surface energy of the deposit. In our case, obviously both cobalt and chromium doping decrease the periphery surface free energy,  $s$ , and the surface free energy of the deposit,  $\sigma$ , and in this way change the surface free energy,  $\Delta\sigma$ . The substrates become hospitable,  $\Delta\sigma < 0$ , for the doped materials. The decrease of the quantity  $\Delta\sigma$  leads to the increase of the temperatures  $T_{34}$  and  $T_{24}$ , while the decrease of the quantity  $s$  leads to a decrease in the nucleation rate. The X-ray investigations indicate that doping with cobalt stimulates the CsCl-type phase growth more than doping with chromium. On the other hand, the films doped with cobalt are thinner than the undoped and chromium doped films, although grown under identical technological conditions. Thus it can be concluded that the doping with cobalt atoms has the effect of further decreasing the surface free energies of the periphery and the deposit. To demonstrate the influence of the two types of doping atoms on the nucleation rate, the nucleation rate temperature dependences were calculated with two different values of  $s$  and  $\Delta\sigma < 0$  according to Equation 1 with  $U = 0$ . Fig. 6a and b show the com-

parison between the nucleation rate temperature dependences for PbTe phases in the undoped films (curves 2, 3, 4 with  $\Delta\sigma = 0$  and  $U = 0$ ), and doped with chromium (curves 2a, 3a, 4a with  $U = 0$ ) and cobalt (curves 2b, 3b, 4b with  $U = 0$ ). Curves 2a, 3a and 4a in Fig. 6a were calculated with  $\Delta\sigma_{Cr} < 0$  and  $s_{Cr} < s$  compared with the undoped films. Curves 2b, 3b and 4b in Fig. 6b were calculated with  $\Delta\sigma_{Co} < \Delta\sigma_{Cr}$  and  $s_{Co} < s_{Cr}$ . It is seen from the figures that the lower the deposit surface free energy, the higher are the temperatures  $T_{34}$  and  $T_{24}$ . Thus the sublayers with the metastable phases of these films consist predominantly of the CsCl-type phase at low substrate temperatures. The strong decrease of the periphery free energy, taking place with cobalt doping, reduces the nucleation rate to values which are lower than those of the undoped material.

### 3.2. Influence of the substrate

#### 3.2.1. Influence on the thickness of the metastable phase sublayers

The thickness of the metastable phase sublayers on KCl substrates is about  $0.7 \mu\text{m}$  and further growth is with the stable fcc phase [1], while films grown on  $\text{BaF}_2$ ,  $3.1 \mu\text{m}$  thick, contain almost entirely HP phases [6]. The reflections of the stable fcc phase have negligible intensities compared to those of the metastable phases, see Fig. 3. The thickness of the sublayers with the metastable phases grown on  $\text{BaF}_2$  substrates is obviously about four to five times higher than for the films on KCl substrates. The quantity of the HP phases in the films deposited on KBr substrates is obviously lower than in the films simultaneously deposited on KCl substrates. The quantity of the HP phases in the films deposited on glass substrates is negligible.

The substrate type can influence the growth mechanism through the kinetic term  $\exp(-U/kT)$ . This term can be ignored in PLE when the linear thermal expansion coefficients of the substrate and the deposited material are equal and have the same temperature behaviour. The high speed of the evaporated material and the comparatively cold substrate make further motion or rotation of the condensed particles practically impossible. This is the case for the films grown on  $\text{BaF}_2$  substrates. As is seen from Fig. 1, the linear expansion coefficient,  $\alpha$ , of PbTe and  $\text{BaF}_2$  are nearly the same. The term  $\exp(-U/kT)$  cannot be ignored in the case of KBr and KCl substrates, which have significantly higher thermal expansion coefficients than PbTe and moreover they change in the temperature range under consideration. To illustrate the influence of the kinetic term, the nucleation rate temperature dependences of the three PbTe phases are calculated according to Equation 1 with  $\Delta\sigma = 0$  and are shown in Fig. 7 with curves 4c, 3c and 2c for the CsCl-type, GeS-type and fcc phases, respectively. In the figure, curves 2, 3 and 4, calculated according to Equation 1 with  $U = 0$  and  $\Delta\sigma = 0$ , are given for comparison. It is clear from Fig. 7, that the difference between the thermal expansion coefficients of the substrate and the deposit leads to a decrease of the

nucleation rate. Fig. 7 explains why the sublayers with metastable phases are thinner in the films grown on KCl and KBr than in those on BaF<sub>2</sub> substrates.

### 3.2.2. Influence on the nucleation rate through the quantity $N_0$ in Equation 1

The density of the absorption sites on the substrate,  $N_0$ , is different for the (1 1 1)-oriented BaF<sub>2</sub> substrate and (100)-oriented KCl and KBr substrates, having different lattice parameters as well. The calculation of the density of the absorption sites gives the following:  $(N_0)_{\text{BaF}_2} = 6.0 \text{ nm}^{-2} > (N_0)_{\text{KCl}} = 5.1 \text{ nm}^{-2} > (N_0)_{\text{KBr}} = 4.6 \text{ nm}^{-2}$ . Thus the quantity  $N_0$  also contributes to the higher nucleation rate of growth on BaF<sub>2</sub> substrate.

The structural investigations indicate that the volume of the CsCl-type phase which grows adjacent to the substrate depends on the substrate type. The volume is smallest in the films grown on BaF<sub>2</sub> substrate where the density of the absorption sites is highest. The volume of the grown solid phase is governed by the substrate type through the density of the absorption sites.

### 3.3. Growth mechanism nature

The structural investigations show that the lattice constants of the metastable phases are smallest in the films grown on BaF<sub>2</sub> substrates. On the other hand, the growth orientation does not depend on the substrate type and orientation. The CsCl-type metastable phase, growing adjacent to the substrate, crystallizes with (100) orientation on both (100)-oriented KCl and KBr and (1 1 1)-oriented BaF<sub>2</sub> substrates. Obviously the (100) direction of crystallization is a thermodynamically favourable growth direction for the CsCl-type phase of PbTe. In our case, as in the case of graphoepitaxy, the film crystal orientation is governed by the growing material symmetry and the corresponding thermodynamically favourable crystallization direction, but not by the substrate relief symmetry. The same holds for further growth. The predominant growth orientation of the polycrystal GeS-type phase seems to be (1 1 1). The upper stable fcc phase always grows with (100) orientation, independently of the nature of the already grown layer ((100) CsCl-type or polycrystal GeS-type phases).

By definition [15], graphoepitaxy is oriented film growth affected by a substrate periodic relief of arbitrary origin. The periodic relief in the case of the monocrystal substrates originates from their periodic potentials. The presence of this relief leads to a decrease of the kinetic term  $\exp(-U/kT)$ . In the case of amorphous glass substrates, the lack of relief symmetry makes the term  $\exp(-U/kT)$  much more significant. Neither of the metastable phases are seen in the film deposited at  $T_s = 250^\circ\text{C}$  and only the GeS-type phase seems to be present in the film grown at  $T_s = 150^\circ\text{C}$  (Fig. 5). Thus, the growth mechanism of

laser-deposited PbTe films on oriented substrates is graphoepitaxy.

## 4. Conclusions

The structural investigations of a number of undoped and doped PbTe films grown by PLE on different types of substrates have been considered in the framework of the general crystallization theory. Although qualitative, these considerations lead to the following conclusions.

1. The influence of doping consists in the change of the surface free energy of the deposited material. This change depends on the amount and type of dopant, and by varying these the relative quantities of the metastable phases in the films can be significantly varied.

2. The substrate type is considered to influence the nucleation rate, and in this way, the relative quantities of the metastable phases through the kinetic term. This term depends on the values and the temperature behaviour of the linear thermal expansion coefficients of the substrate and the deposit.

3. The growth mechanism in the process of PLE is graphoepitaxy. The relief symmetry due to the potential periodicity of the monocrystal substrates stimulates the film growth without determining the crystallization direction. All three PbTe phases grow in their thermodynamically favourable directions of crystallization.

## References

1. M. BALEVA, L. BOZUKOV and E. TZUKEVA, *Semicond. Sci. Technol.* **8** (1993) 1208.
2. Y. FUJII, K. KITAMURA, A. ONODERA and Y. YAMADA, *Solid State Commun.* **49** (1984) 135.
3. T. CHATTOPADHYAY, A. WERNER and H. VON SCHERING, "Materials Research Society Proceedings", Vol. 22 (Elsevier Science, Amsterdam, 1984).
4. T. CHATTOPADHYAY, H. VON SCHERING, W. GRESSHAUS and W. HOLZAPFEL, *Phys. B + C* **139-40** (1986) 356.
5. M. BALEVA and E. MATEEVA, *Phys. Rev. B* **48** (1993) 2659.
6. *Idem, ibid.* **50** (1994) 8893.
7. M. BALEVA, E. MATEEVA and M. MOMTCHILOVA, *J. Phys. Condens. Matter* **4** (1992) 8997.
8. M. BALEVA, E. MATEEVA, M. PETRAUSKAS, R. TOMASIUNAS and R. MASTEIKA, *ibid.* **4** (1992) 9009.
9. M. BALEVA and E. MATEEVA, *ibid.* **5** (1993) 7970.
10. M. BALEVA, M. MAKSIMOV, S. METEV and M. SENDOVA, *J. Mater. Sci. Lett.* **5** (1986) 533.
11. E. VORONKOVA, B. GRECHUSHNIKOV, G. DISTLER and I. PETROV, "Optical Materials for IR technique" (Nauka, Moscow, 1965) in Russian.
12. R. DALVEN, *Infrared Phys.* **9** (1969) 141.
13. L. ESKERTOVA, "Physics of thin films" (Plenum, New York, London, SNTL Publishers of Technical Literature, Prague, 1986) p. 103.
14. D. KASHCHIEV, *J. Cryst. Growth* **40** (1977) 29.
15. E. GIVARGIZOV, "Artificial Epitaxy" (Nauka, Moscow, 1988) in Russian.

Received 21 March  
and accepted 8 September 1995